

# The Gravitational Bending of Acoustic Schwarzschild Black Hole

Chen-Kai Qiao<sup>\*</sup> and Mi Zhou<sup>†</sup>

*College of Science, Chongqing University of Technology, Banan, Chongqing, 400054, China*

(Dated: December 26, 2023)

Acoustic black hole is becoming an attractive topic in recent years, for it open-up new direction for experimental explorations of black holes. In this work, the gravitational bending of acoustic Schwarzschild black hole is investigated. We resort to the approach developed by Gibbons and Werner, in which the gravitational deflection angle is calculated using the Gauss-Bonnet theorem in geometrical topology. In this approach, the gravitational bending is directly connected with the topological properties of curved spacetime. In this work, the gravitational deflection angle of light, weak gravitational lensing and Einstein ring for acoustic Schwarzschild black hole are carefully studied and analyzed. The results show that the gravitational bending effects in acoustic Schwarzschild black hole are enhanced, compared with those in conventional Schwarzschild black hole. This observation indicates that the acoustic black holes may be more easily detectable in gravitational bending and weak gravitational lensing observations.

Keywords: Gravitational Bending; Gauss-Bonnet Theorem; Acoustic Schwarzschild Black Hole

## I. INTRODUCTION

Gravitational bending is one of the most important phenomenon predicted by Einstein's general theory of relativity. This prediction was first observed in 1919 by A. S. Eddington *et al.* as a demonstration of general relativity [1]. As significant application of gravitational bending, the weak gravitational lensing is becoming an important tool in astronomy and cosmology [2, 3]. The gravity theories and astrophysical models can be tested experimentally from these gravitational bending and weak gravitational lensing observations. Further, the dark matter distribution in galaxies can also be revealed from gravitational lensing [4]. In the past decades, the gravitational bending effect and gravitational lensing become crucial points in physics and astronomy [2–5].

Black hole, since it was proposed, has attracted great interests in high-energy physics, astrophysics and astronomy. Significantly important information on gravitation, thermodynamics and quantum effects in curved spacetime can be revealed through black holes [6]. For a long time, researches on black holes were mainly motivated by theories. However, huge progresses on experimental explorations of black holes have been witnessed in recent years. The gravitational wave signals were detected by LIGO and Virgo from the merging of binary black holes [7]. The first black hole image at the center of galaxy M87 was observed by Event Horizon Telescope in 2019 [8].

Besides the astrophysical side, many investigations on black holes also take place in other branches of physics. The emergence of acoustic black hole is one of such attempts. Historically, acoustic black hole was first proposed by W. G. Unruh to provide connection between

astrophysical black holes and tabletop experiments [9]. These kind of black holes can be formed by moving fluid with speed faster than the local sound speed. The behavior of fluid eventually generate an analogue gravity model and form an effective curved spacetime. The acoustic black holes and corresponding analogue gravity models become extremely useful in quantum physics, high-energy physics and condensed matter physics [10]. The interplay between black holes and quantum particles, as well as their quantum gravitational effects, could be mimicked by such kind of black holes [11–13]. There are a number of progresses in this area in the past years. Experimentally, the acoustic black hole was first reported in Bose-Einstein condensate system [14]. And similar experimental realization of acoustic black holes also emerged in other systems [15–18]. Remarkably, the analogue Hawking radiation and its Hawking temperature of acoustic black holes were also successfully realized in experiments [16, 19, 20]. With these superiorities, acoustic black holes and corresponding analog gravity models have great impact on theoretical as well as experimental physics.

The acoustic black holes have extremely rich properties in nature. Because of the equivalent mathematical descriptions between astrophysical black holes and acoustic black holes, it can be conjectured that, if a physical phenomenon happens in an astrophysical black hole scenario, it may also occur in acoustic black holes and analogue gravity models. Recently, the acoustic black holes have attracted large number of interests. Many kinds of acoustic black holes have been constructed by fluid systems propagating in flat or curved spacetime background [10, 11, 21–24]. These acoustic black holes not only can be produced in condensed matter systems, but also could be generated by mechanisms in high-energy physics and cosmology. In 2019, X.-H. Ge *et al.* obtained a class of acoustic black hole solutions for analog gravity models by considering the relativistic Gross-Pitaevskii

<sup>\*</sup> chenkaicao@cqut.edu.cn

<sup>†</sup> lilyzm@cqut.edu.cn

and Yang-Mills theories [24]. Furthermore, the horizons, shadows, quasinormal modes, quasibound states, Hawking radiations, Unruh effect, quasiparticle propagation and deflection for acoustic black holes are studied and analyzed systematically [25–33].

In this paper, we study the gravitational bending of light in spacetime generated by acoustic black holes. A simple and representative example, the acoustic Schwarzschild black hole, is chosen in this work to show the gravitational bending effect of acoustic black holes. Similar to the conventional Schwarzschild black hole in general relativity, the acoustic Schwarzschild black hole could also reveal some universal properties of the more complex acoustic black holes. A comprehensive understanding of such black hole could provide useful information and profound insights for many acoustic black holes.

In the present work, the gravitational deflection angle of light, weak gravitational lensing, Einstein rings of acoustic Schwarzschild black hole are carefully studied and analyzed in details. Hopefully, the conclusions generated from acoustic Schwarzschild black hole could give hints for more complex acoustic black holes and the various analogue gravity models.

In the study of gravitational bending effects, we adopt the approach developed by G. W. Gibbons and M. C. Werner [34], in which the gravitational deflection angle of light in curved spacetime is determined by geometric and topological methods. In their approach, the gravitational deflection angle is calculated by applying Gauss-Bonnet theorem in optical reference metric / optical manifold. From this approach, the gravitational deflection angle of light is directly connected with the topological properties of curved spacetime. Therefore, the Gauss-Bonnet theorem can give us new insights on gravitational bending effects. It would be a promising tool in dueling with gravity problems. Recently, Gibbons and Werner's approach has been applied to many gravitational systems, and consistent results with traditional methods have been obtained [35–43]. Furthermore, some studies suggested that, apart from light bending, the gravitational bending effects for charged particles near massive objects can also be correctly handled using Gauss-Bonnet theorem [45–48].

This paper is organized as follows: Section I gives an introduction of this work. Section II briefly describes the Gauss-Bonnet theorem in geometrical topology. The approach developed by Gibbons and Werner, in which the gravitational deflection angle of light is calculated using Gauss-Bonnet theorem, is also introduced in this section. The acoustic Schwarzschild black hole is reviewed in section III. Section IV is devoted to the gravitational bending effect of acoustic Schwarzschild black hole. Results and discussions on gravitational deflection angle of light, weak gravitational lensing and Einstein ring are presented in this section. Summary and conclusions are given in section V. In this work, the natural unit  $G = c = 1$  is adopted.

## II. GAUSS-BONNET THEOREM AND ITS APPLICATION ON GRAVITATIONAL BENDING

Gauss-Bonnet theorem is one of the most significant theorems in differential geometry and geometrical topology. It provide connections between geometry and topology in curved manifold [49]. In Gauss-Bonnet theorem, topological properties of curved manifold, such as the Euler characteristic number, are reflected by pure geometric quantities (namely the various curvatures). Particularly, in a 2-dimensional curved manifold, the mathematical description of Gauss-Bonnet theorem is

$$\int_D \mathcal{K} dS + \int_{\partial D} \kappa_g dl + \sum_{i=1}^N \theta_i = 2\pi \chi(D) \quad (1)$$

Here,  $D$  is a region in curved manifold,  $\mathcal{K}$  is the Gauss curvature,  $\kappa_g$  is the geodesic curvature of boundary  $\partial D$ ,  $\chi(D)$  is the Euler characteristic number for region  $D$ , and  $\theta_i$  is the exterior angle for each discontinuous point of boundary  $\partial D$ . In a regular and simply-connected region  $D$  without singularities, Euler characteristic number becomes  $\chi(D) = 1$ .

In 2008, G. W. Gibbons and M. C. Werner developed a new approach to calculate the gravitational deflection angle of light using Gauss-Bonnet theorem [34]. In this approach, the gravitational deflection angle of light can be reflected by topological properties of curved spacetime, therefore it gives new insights on gravitational bending effects. Recently, this approach has been applied to many gravitational systems, and consistent results with traditional methods have been obtained [35–42].

In Gibbons and Werner's work, the gravitational deflection angle is calculated by applying Gauss-Bonnet theorem in optical reference metric / optical manifold. For a 4-dimensional asymptotically flat and spherical symmetric spacetime

$$\begin{aligned} d\tau^2 &= g_{\mu\nu} dx^\mu dx^\nu \\ &= f(r) dt^2 - \frac{1}{f(r)} dr^2 - r^2 (d\theta^2 + \sin^2 \theta d\phi^2) \end{aligned} \quad (2)$$

the optical reference metric gives a 3-dimensional Riemannian manifold

$$\begin{aligned} dt^2 &= g_{ij}^{\text{OP}} dx^i dx^j \\ &= \frac{1}{f(r)} \left[ \frac{1}{f(r)} dr^2 + r^2 d\theta^2 + r^2 \sin^2 \theta d\phi^2 \right] \end{aligned} \quad (3)$$

Actually, this optical reference metric is obtained from the 3-dimensional sub-manifold of the 4-dimensional spacetime by imposing the null constrain  $d\tau^2 = 0$ . This 3-dimensional sub-manifold is also called as optical manifold or optical geometry in literature [50, 51]. The propagation of light beams, which is along null geodesic in original 4-dimensional spacetime manifold, still maintains geodesic in optical reference manifold. Since the

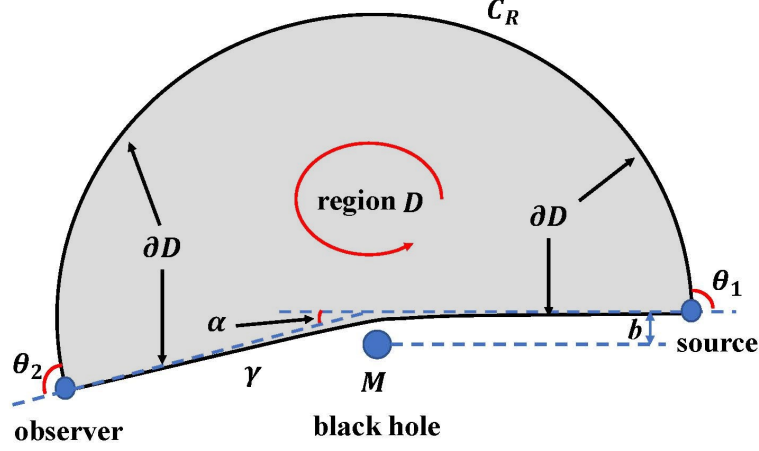


FIG. 1. Calculating the gravitational deflection angle of light using the Gauss-Bonnet theorem. This figure shows the choice of region  $D$  in the equatorial plane of optical manifold for asymptotically flat spacetime, which makes the application of Gauss-Bonnet theorem in equation (1) available. The direction of boundary  $\partial D$  in the contour integral  $\int_{\partial D} \kappa_g dl$  is chosen to be counterclockwise. Note that for photon orbit  $\gamma$ , this choice of direction (which is from observer to light source) is opposite to the light propagation.

spacetime in equation (2) is spherical symmetric, without loss of generality, we can restrict the above optical manifold (as well as the optical reference metric  $g_{ij}^{\text{OP}}$ ) in the equatorial plane. In this way, a 2-dimensional Riemannian manifold is eventually obtained, and the application of Gauss-Bonnet theorem in equation (1) becomes available.

In the calculations, the region  $D$  in Gauss-Bonnet theorem is chosen in the following way. For asymptotically flat spacetime, when light source and observer are both very far from the central massive black hole,  $D$  is a simply connected region in equatorial plane such that the light source and observer are connected by its boundary  $\partial D$ . The boundary  $\partial D$  is generated by two parts: a photon orbit  $\gamma$  from light source to observer, and a circular arc  $C_R$  connected with the source and observer. The central black hole is located outside the region  $D$ , so that spacetime singularities are excluded from  $D$ . This region is schematically illustrated in figure 1.

For the picked region  $D$  in figure 1, the exterior angles for discontinuous points of boundary  $\partial D$  are  $\theta_1 \approx \theta_2 \approx \pi/2$ . Therefore, in the Gauss-Bonnet theorem, we have

$$\sum_{i=1}^N \theta_i = \theta_1 + \theta_2 \approx \pi \quad (4)$$

The boundary  $\partial D$  in figure 1 consists of two parts: the photon orbit  $\gamma$  and the outer circular arc  $C_R$ . Further, if the observer and light source are both very far from the central massive black hole, we can simply use the limit  $R \rightarrow \infty$ . Because the photon orbit in gravitational field is a geodesic curve in optical geometry, its geodesic cur-

vature  $\kappa_g(\gamma)$  vanishes. Then the contour integral reduces to

$$\begin{aligned} \int_{\partial D} \kappa_g dl &= \int_{\gamma} \kappa_g(\gamma) dl + \lim_{R \rightarrow \infty} \int_{C_R} \kappa_g(C_R) dl \\ &= \lim_{R \rightarrow \infty} \int_{C_R} \kappa_g(C_R) dl \end{aligned} \quad (5)$$

For asymptotically flat spacetime, many studies have shown that the integration of geodesic curvature  $\kappa_g$  along circular arc  $C_R$  in  $R \rightarrow \infty$  limit reduces to [52, 59]

$$\int_{\partial D} \kappa_g dl = \lim_{R \rightarrow \infty} \int_{C_R} \kappa_g(C_R) dl \approx \pi + \alpha \quad (6)$$

where  $\alpha$  is the gravitational deflection angle of light.

Combining the exterior angle in equation (4), geodesic curvature in equation (6) and Euler characteristic number  $\chi(D) = 1$ , the Gauss-Bonnet theorem in equation (1) leads to

$$\begin{aligned} \int_D \mathcal{K} dS + \int_{\partial D} \kappa_g dl + \sum_{i=1}^N \theta_i &= \int_D \mathcal{K} dS + (\pi + \alpha) + \pi \\ &= 2\pi\chi(D) = 2\pi \end{aligned} \quad (7)$$

Therefore, the gravitational deflection angle of light can be calculated through

$$\alpha = - \int_D \mathcal{K} dS \quad (8)$$

This is the gravitational deflection angle of light for spherical symmetric and asymptotically flat spacetime.

These results correspond to the cases where observer and light source are both from infinity (namely both observer and light source are very far from the central massive black hole). When light source and observer are located at finite distance region, the algorithm is presented in Appendix A.

### III. ACOUSTIC SCHWARZSCHILD BLACK HOLE

Acoustic black holes can be proposed in several ways [9, 11, 21–24], not only from laboratory tabletop experiments in condensed matter systems, but also from mechanisms in high-energy physics and cosmology. In a recent work, X.-H. Ge *et al.* obtained a class of acoustic black hole solutions using the relativistic Gross-Pitaevskii and Yang-Mills theories [24].

In this section, we choose the acoustic black holes generated in Gross-Pitaevskii theory to shown Ge’s formulation. In Gross-Pitaevskii theory, the action is given by [54]

$$S = \int d^4x \sqrt{-g} \left( |\partial_\mu \varphi|^2 + m^2 |\varphi|^2 - \frac{b}{2} |\varphi|^4 \right) \quad (9)$$

Here,  $m^2 \sim (T - T_C)$  is a parameter depending on the temperature of fluid system,  $b$  is a constant, and  $\varphi$  is a complex scalar field expressed as  $\varphi = \sqrt{\rho(\vec{x}, t)} \exp i\hat{\theta}(\vec{x}, t)$ . The complex scalar field  $\varphi$  corresponds to the order parameter in the phase transition of fluid system, and it propagates in a static background spacetime

$$ds_{\text{background}}^2 = g_{tt} dt^2 + g_{rr} dr^2 + g_{\theta\theta} d\theta^2 + g_{\phi\phi} d\phi^2 \quad (10)$$

Here,  $g_{tt}$ ,  $g_{rr}$ ,  $g_{\theta\theta}$  and  $g_{\phi\phi}$  is the metric of background spacetime. After some calculations and rearrangements of parameters, the propagation of the phase fluctuation  $\hat{\theta}$  in complex scalar field  $\varphi$  can be expressed using the wave propagation equation in curved spacetime

$$\frac{1}{\sqrt{-G}} \partial_\mu (\sqrt{-G} G^{\mu\nu} \partial_\nu \hat{\theta}) = 0 \quad (11)$$

In this equation,  $G_{\mu\nu}$  is the effective spacetime metric tensor describing the phase fluctuation propagation in fluid systems.

$$\begin{aligned} ds^2 &= G_{\mu\nu} dx^\mu dx^\nu \\ &= c_s \sqrt{c_s^2 - v_\mu v^\mu} \cdot \left[ \frac{c_s^2 - v_r v^r}{c_s^2 - v_\mu v^\mu} g_{tt} dt^2 \right. \\ &\quad \left. + \frac{c_s^2}{c_s^2 - v_r v^r} g_{rr} dr^2 + g_{\theta\theta} d\theta^2 + g_{\phi\phi} d\phi^2 \right] \quad (12) \end{aligned}$$

The definition of  $c_s$  and  $v_\mu$  can be found in references [24, 31]. From the above equation, it is obvious that the behavior of phase fluctuation propagation in fluid system

is peculiar, as if it was lived in a curved spacetime. Therefore, we can effectively give a mathematical description of black hole spacetime to the fluid system. In this way, the spacetime metric of acoustic black hole is generated.

In this work, we are interested in a typical and simple acoustic black hole, the acoustic Schwarzschild black hole. From Ge’s formulation, it can be generated by fluid propagating in Schwarzschild background. The spacetime metric for acoustic Schwarzschild black hole is

$$\begin{aligned} d\tau^2 &= G_{\mu\nu} dx^\mu dx^\nu \\ &= f(r) dt^2 - \frac{1}{f(r)} dr^2 - r^2 (d\theta^2 + \sin^2 \theta d\phi^2) \quad (13) \end{aligned}$$

where function  $f(r)$  is defined as:

$$f(r) = \left( 1 - \frac{2M}{r} \right) \cdot \left[ 1 - \xi \frac{2M}{r} \left( 1 - \frac{2M}{r} \right) \right] \quad (14)$$

Here,  $\xi$  is the tuning parameter. It is closely connected to the radial velocity of moving fluid, via  $v_r = \sqrt{2M\xi/r}$ . For the fluid velocity  $v_r$  to be real, tuning parameter must satisfies  $\xi \geq 0$ . When  $\xi = 0$ , the above spacetime reduces to the conventional Schwarzschild black hole. When  $\xi \rightarrow +\infty$ , the whole spacetime ( $0 \leq r \leq +\infty$ ) is inside the acoustic black hole [31]. Similar to the conventional Schwartzschild black hole in general relativity, the acoustic Schwartzschild black hole may also reflect some universal properties of more complex acoustic black holes. A comprehensive understanding of such black hole could provide useful information and profound insights for many acoustic black holes.

The horizon of acoustic Schwarzschild black hole is determined via equation

$$\begin{aligned} f(r) &= \left( 1 - \frac{2M}{r} \right) \cdot \left[ 1 - \xi \frac{2M}{r} \left( 1 - \frac{2M}{r} \right) \right] \\ &= (r - r_s)(r - r_{ac-})(r - r_{ac+}) = 0 \quad (15) \end{aligned}$$

Here,  $r_s = 2M$  is the “optical” event horizon, while  $r_{ac-} = M(\xi - \sqrt{\xi^2 - 4\xi})$  and  $r_{ac+} = M(\xi + \sqrt{\xi^2 - 4\xi})$  are the “interior” and “exterior” acoustic event horizons respectively [32]. The necessary condition for the existence of acoustic event horizon is  $\xi \geq 4$ . When tuning parameter satisfies  $0 \leq \xi < 4$ , only “optical” horizon exists in acoustic Schwarzschild black hole, Both “interior” and “exterior” acoustic event horizons disappear in this case. When tuning parameter  $\xi = 4$ , the “interior” and “exterior” acoustic event horizons coincide with each other, and we get the extreme acoustic Schwarzschild black hole. When tuning parameter  $\xi > 4$ , there are three interesting regions in acoustic Schwarzschild black hole. In region  $r < r_s$ , both light rays (photons) and sound waves (phonons) cannot escape from the acoustic black hole. In region  $r_s < r < r_{ac+}$ , light rays could escape from acoustic black hole, while sound waves cannot. In region  $r > r_{ac+}$ , both light rays and sound waves could escape from the acoustic black hole.

#### IV. GRAVITATIONAL BENDING EFFECTS FOR ACOUSTIC SCHWARZSCHILD BLACK HOLE: RESULTS AND DISCUSSIONS

In this section, the gravitational bending effect of acoustic Schwarzschild black hole is analyzed in details. Results and discussions on gravitational deflection angle of light, lens equation and Einstein ring are presented. In subsection IV A, the gravitational deflection angle of light is calculated using Gauss-Bonnet theorem. Subsection IV B presents results on weak gravitational lensing and Einstein Ring of acoustic Schwarzschild black hole.

##### A. Gravitational Deflection Angle of Light

This subsection presents results and discussions of the deflection angle in cases where light source and observer are located at infinity. Moreover, the gravitational deflection angle in cases where light source and observer are located at finite distance region is presented in Appendix A.

To apply the Gauss-Bonnet theorem in equation (1), we should firstly get the optical reference metric for curved spacetime. The optical reference metric for acoustic Schwarzschild black hole can be derived from the null constrain ( $d\tau^2 = 0$ ). In this way, the explicit form of optical reference metric is

$$dt^2 = g_{ij}^{\text{OP}} dx^i dx^j = \frac{1}{f(r)} \left[ \frac{1}{f(r)} dr^2 + r^2 d\theta^2 + r^2 \sin^2 \theta d\phi^2 \right] \quad (16)$$

Here,  $f(r)$  is defined in equation (14), the Greek indices  $\mu, \nu$  run over 0,1,2,3; while the Latin indices  $i, j, k$  run over 1,2,3, respectively. Since the optical geometry in equation (16) is spherical symmetric, without loss of generality, we can restrict light rays to the equatorial plane, in which the polar angle is fixed at  $\theta = \pi/2$ . In this way, the optical reference metric for acoustic Schwarzschild black hole restricted in equatorial plane can be expressed as:

$$dt^2 = \tilde{g}_{ij}^{\text{OP}} dx^i dx^j = \frac{1}{[f(r)]^2} dr^2 + \frac{r^2}{f(r)} d\phi^2 \quad (17)$$

In the equatorial plane of optical manifold, the Gauss curvature with respect to optical metric can be calculated with the help of Riemannian geometry [55]

$$\begin{aligned} \mathcal{K} &= -\frac{1}{\sqrt{\tilde{g}^{\text{OP}}}} \left[ \partial_\phi \left( \frac{\partial_\phi (\sqrt{\tilde{g}_{rr}^{\text{OP}}})}{\sqrt{\tilde{g}_{\phi\phi}^{\text{OP}}}} \right) + \partial_r \left( \frac{\partial_r (\sqrt{\tilde{g}_{\phi\phi}^{\text{OP}}})}{\sqrt{\tilde{g}_{rr}^{\text{OP}}}} \right) \right] = \frac{1}{2} f(r) \cdot \frac{d^2 f(r)}{dr^2} + \frac{1}{2} \left[ \frac{df(r)}{dr} \right]^2 \\ &= -\frac{2M(1+\xi)}{r^3} + \frac{3M^2(\xi^2 + 10\xi + 1)}{r^4} - \frac{48M^3\xi(\xi + 2)}{r^5} + \frac{8M^4\xi(27\xi + 11)}{r^6} - \frac{384M^5\xi^2}{r^7} + \frac{240M^6\xi^2}{r^8} \end{aligned} \quad (18)$$

And the surface area in the equatorial plane can be expressed as

$$\begin{aligned} dS &= \sqrt{\tilde{g}^{\text{OP}}} dr d\phi = \frac{r}{[f(r)]^{3/2}} dr d\phi = \frac{r dr d\phi}{\left\{ \left( 1 - \frac{2GM}{r} \right) \cdot \left[ 1 - \xi \frac{2GM}{r} \left( 1 - \frac{2GM}{r} \right) \right] \right\}^{3/2}} \\ &= \left[ 1 + \frac{3M(1+\xi)}{r} + \frac{3M^2(5\xi^2 + 2\xi + 5)}{2r^2} + \frac{M^3(35\xi^3 - 15\xi^2 + 9\xi + 35)}{2r^3} + \frac{15M^4(21\xi^4 - 28\xi^3 - 2\xi^2 + 4\xi + 21)}{8r^4} \right. \\ &\quad \left. + \frac{3M^5(231\xi^5 - 525\xi^4 + 70\xi^3 - 10\xi^2 + 35\xi + 231)}{8r^5} + o\left(\frac{M^6}{r^6}\right) \right] r dr d\phi \end{aligned} \quad (19)$$

In the calculation of gravitational deflection angle for acoustic Schwarzschild black hole, we choose the region  $D$  in figure 1 to apply the Gauss-Bonnet theorem. It is a simply connected region with light source and observer connected by its boundary  $\partial D$ . The central black hole is located outside  $D$ , so that the spacetime singularity of black hole is excluded from  $D$ . The boundary  $\partial D$  in figure 1 consists of two parts: the photon orbit  $\gamma$  and the outer circular arc  $C_R$ . The photon orbit  $\gamma$  is a geodesic curve in the optical manifold, so its geodesic vanishes  $\kappa_g(\gamma) = 0$ . For outer circular arc  $C_R$ , its geodesic curvature can be expressed using the geodesic curvature formula for constant radius curve [55]

$$\kappa_g(C_R) = \frac{1}{2\sqrt{\tilde{g}_{rr}^{\text{OP}}}} \frac{\partial \tilde{g}_{\phi\phi}^{\text{OP}}}{\partial r} = \frac{f(r)}{r} - \frac{1}{2} \frac{\partial f(r)}{\partial r} = \frac{1}{r} - \frac{3M(1+\xi)}{r^2} + \frac{16M^2\xi}{r^3} - \frac{20M^3\xi}{r^4} \quad (20)$$



Combining the above results, the integration of geodesic curvature  $\kappa_g$  along the boundary  $\partial D$  becomes

$$\begin{aligned}
\int_{\partial D} \kappa_g dl &= \lim_{R \rightarrow \infty} \int_{C_R} \kappa_g(C_R) dl = \lim_{R \rightarrow \infty} \int_{\phi_{\text{source}}}^{\phi_{\text{observer}}} \kappa_g(C_R) R d\phi \\
&\approx \lim_{R \rightarrow \infty} \int_0^{\pi+\alpha} \kappa_g(C_R) R d\phi \\
&= \lim_{R \rightarrow \infty} \int_0^{\pi+\alpha} \left[ \frac{1}{R} - \frac{3M(1+\xi)}{R^2} + \frac{16M^2\xi}{R^3} - \frac{20M^3\xi}{R^4} \right] R d\phi \\
&= \pi + \alpha
\end{aligned} \tag{21}$$

Because the light source and observer are both located at infinite distance, so the approximations  $\phi_{\text{source}} \approx 0$  and  $\phi_{\text{observer}} \approx \pi + \alpha$  can be used, as indicated in figure 1. Note that this result is consistent with equation (6) obtained in many literatures [52, 59]. The spacetime generated by acoustic Schwarzschild black hole is a asymptotically flat spacetime. For this kind of spacetime, the geodesic curvature in equatorial plane of outer circular arc  $C_R$  approaches to  $\kappa_g(C_R) \rightarrow 1/R$  when  $R \rightarrow \infty$ , and the contour integral reduces to  $\int_{C_R} \kappa_g(C_R) dl \approx \pi + \alpha$  [52, 59]. As explained in figure 1, the direction of boundary  $\partial D$  in the contour integral  $\int_{\partial D} \kappa_g dl$  in equation (21) is chosen to be counterclockwise. For photon orbit  $\gamma$ , this choice of direction (which is from observer to light source) is opposite to the light propagation.

For region  $D$ , the exterior angles for discontinuous points of boundary  $\partial D$  are determined in figure 1

$$\theta_1 \approx \theta_2 \approx \pi/2 \Rightarrow \sum_{i=1}^N \theta_i = \theta_1 + \theta_2 \approx \pi \tag{22}$$

Further, the Euler characteristic number for simply connected region  $D$  is  $\chi(D) = 1$ . By applying the Gauss-Bonnet theorem in equation (1), the gravitational deflection angle of light in acoustic Schwarzschild black hole can be obtained

$$\begin{aligned}
\int_D \mathcal{K} dS + \int_{\partial D} \kappa_g dl + \sum_{i=1}^N \theta_i &= \int_D \mathcal{K} dS + (\pi + \alpha) + \pi = 2\pi\chi(D) = 2\pi \\
\Rightarrow \alpha &= - \int_D \mathcal{K} dS = - \int_{\phi_{\text{source}}}^{\phi_{\text{observer}}} d\phi \int_{r(\gamma)}^{\infty} \mathcal{K} \frac{r}{[f(r)]^{3/2}} dr
\end{aligned} \tag{23}$$

To evaluate the integral, the radius of photon orbit  $r(\gamma) = r(\phi)$  must be determined. In principle, the exact value of  $r(\gamma)$  is calculated by solving the differential equation for null geodesic. However, the purpose of Gibbons and Werner's approach is calculating the deflection angle through basic calculus and topological properties, without solving any complicated differential equations. For this purpose, in actual calculations, we can use the leading order perturbation for photon orbit.

$$r(\gamma) = r(\phi) \approx \frac{b}{\sin \phi} \tag{24}$$

Here,  $b$  is impact parameter indicated in figure 1. This is exactly the photon orbit in Newtonian gravity. Furthermore, we also assume that the gravitational deflection angle is not large, which correspond to the weak gravitational lensing. In this case, when light source and observer are located at infinite distance, we have

$$\phi_{\text{source}} \approx 0; \quad \phi_{\text{observer}} \approx \pi + \alpha \approx \pi \tag{25}$$

With  $r(\gamma)$ ,  $\phi_{\text{source}}$  and  $\phi_{\text{observer}}$  obtained, the integration of Gauss curvature can be evaluated.

$$\begin{aligned}
\alpha &= - \int_D \mathcal{K} dS = - \int_{\phi_{\text{source}}}^{\phi_{\text{observer}}} d\phi \int_{r(\gamma)}^{\infty} \mathcal{K} \frac{r}{[f(r)]^{3/2}} dr \\
&\approx - \int_0^\pi d\phi \int_{\frac{b}{\sin \phi}}^{\infty} \mathcal{K} \frac{r}{[f(r)]^{3/2}} dr \\
&= - \int_0^\pi d\phi \int_{\frac{b}{\sin \phi}}^{\infty} \left[ -\frac{2M(1+\xi)}{r^2} - \frac{3M^2(\xi^2 - 6\xi + 1)}{r^3} - \frac{6M^3(\xi - 1)(\xi^2 - 4\xi - 1)}{r^4} + o\left(\frac{M^5}{r^5}\right) \right] dr \\
&= \int_0^\pi \left[ \frac{2M(1+\xi) \sin \phi}{b} + \frac{3M^2(\xi^2 - 6\xi + 1) \sin^2 \phi}{2b^2} + \frac{2M^3(\xi - 1)(\xi^2 - 4\xi - 1) \sin^3 \phi}{b^3} + o\left(\frac{M^4}{b^4}\right) \right] d\phi \\
&= \frac{4M(1+\xi)}{b} + \frac{3M^2(\xi^2 - 6\xi + 1)\pi}{4b^2} + \frac{8M^3(\xi - 1)(\xi^2 - 4\xi - 1)}{3b^3} + o\left(\frac{M^4}{b^4}\right)
\end{aligned} \tag{26}$$

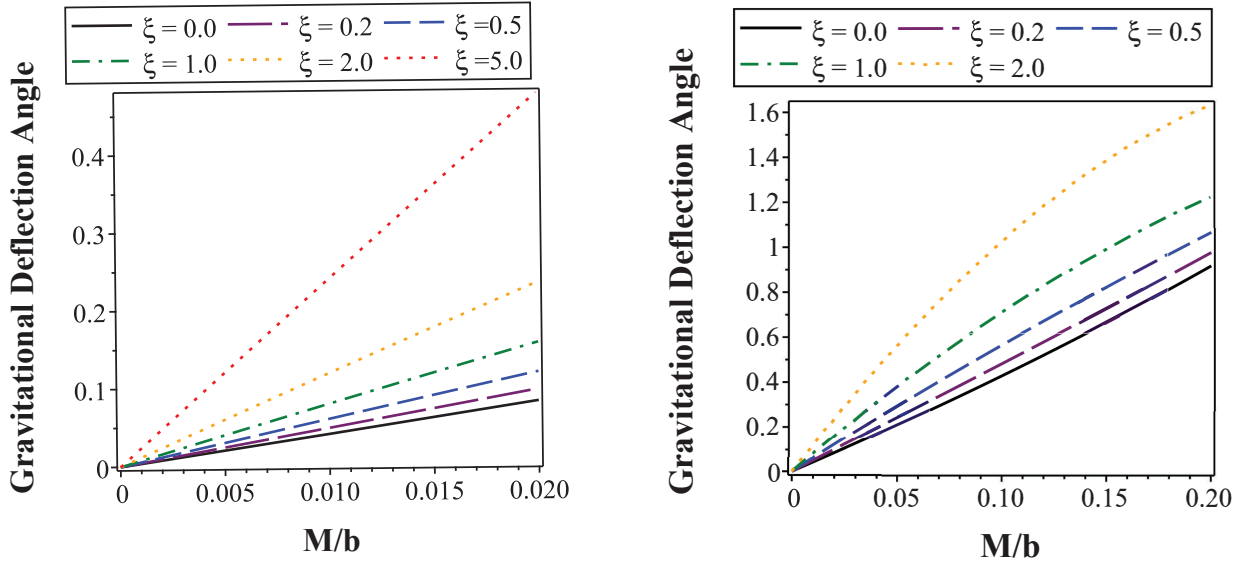


FIG. 2. The gravitational deflection angles of light in acoustic Schwarzschild black hole for several  $\xi$  values. The horizontal axis labels the  $M/b$  and the vertical axis labels the gravitational deflection angle  $\alpha$ . In the left panel, the gravitational deflection angles are plotted in region  $0 \leq M/b \leq 0.02$ . While the deflection angles for larger  $M/b$  ( $0 \leq M/b \leq 0.2$ ) are shown in the right panel. In left panel, the gravitational deflection angles are plotted for tuning parameter  $\xi = 0, 0.2, 0.5, 1, 2, 5$ . While in right panel, the deflection angle for  $\xi = 5$  would be vary large (when  $M/b \sim 0.2$ ,  $\alpha \sim \pi$ ), so we omit this case in the plotting.

The above result in equation (26) is the gravitational deflection angle of light for acoustic Schwarzschild black hole in cases where light source and observer are both located at infinite distance. When the distances between light source, observer and central black hole are finite, the gravitational deflection angle is presented in the Appendix. Detailed calculations confirmed that the above result in equation (26) is consistent with the gravitational deflection angle for finite distance (which is given in equation (A6)). Furthermore, when tuning parameter  $\xi = 0$ , equation (26) exactly reduces to the gravitational deflection angle of light in conventional Schwarzschild spacetime. Recall that the leading order contribution of gravitational deflection angle in Schwarzschild spacetime is

$$\alpha_{\text{Schwarzschild}} = \frac{4M}{b} + o\left(\frac{M^2}{b^2}\right) \quad (27)$$

These observations can demonstrate the validity of the approach and calculations in the present work [56].

However, when tuning parameter  $\xi \neq 0$ , deviations between conventional Schwarzschild black hole and acoustic Schwarzschild black hole emerge, and the gravitational bending behavior may exhibit different features. In figure 2, the gravitational deflection angles of light in acoustic Schwarzschild black hole are presented for several  $\xi$  values. Since the expression of gravitational deflection angle is expressed in power series of  $M/b$ , we mostly focus on the region where  $M/b$  is sufficiently small. These cases correspond to the weak gravitational lensing phenomenon. The left panel of figure 2 shows the gravita-

tional deflection angle in region  $0 \leq M/b \leq 0.02$ . From this figure, it is indicated that the deflection angles in acoustic Schwarzschild black hole are larger than that in conventional Schwarzschild black hole. Moreover, when tuning parameter  $\xi$  increases, the deflection angle  $\alpha$  enlarges. This is because that the deflection angle is mostly dominant by the first term  $4M(1+\xi)/b$  in equation (26). When tuning parameter  $\xi$  is bigger, the deflection angle of light is larger. Therefore, acoustic Schwarzschild black hole with large tuning parameter could greatly intensify the gravitational bending effect of light. The acoustic black holes, with the presence of moving fluids and sound-waves, may be more easily detectable through gravitational bending effect.

To see the strong gravitational bending case for larger  $M/b$ , we also plot the gravitational deflection angle for  $0 \leq M/b \leq 0.2$  in the right panel of figure 2. The non-linearity of deflection angle is clearly exhibited in right panel. This non-linearity is caused by higher order power series of  $M/b$  in equation (26). Furthermore, for large  $M/b$ , the gravitational deflection angle of light could become vary large. For instance, when  $M/b \sim 0.2$ , the deflection angle reaches  $\alpha \sim \pi/2$  for tuning parameter  $\xi = 2$ , and even reaches  $\alpha \sim \pi$  for tuning parameter  $\xi = 5$  (which is not plotted in this figure). In these cases, the approximation  $\phi_{\text{observer}} \approx \pi + \alpha \approx \pi$  used in the integration of Gauss curvature no longer satisfied, and more precise methods are needed to explore the gravitational bending in this region.

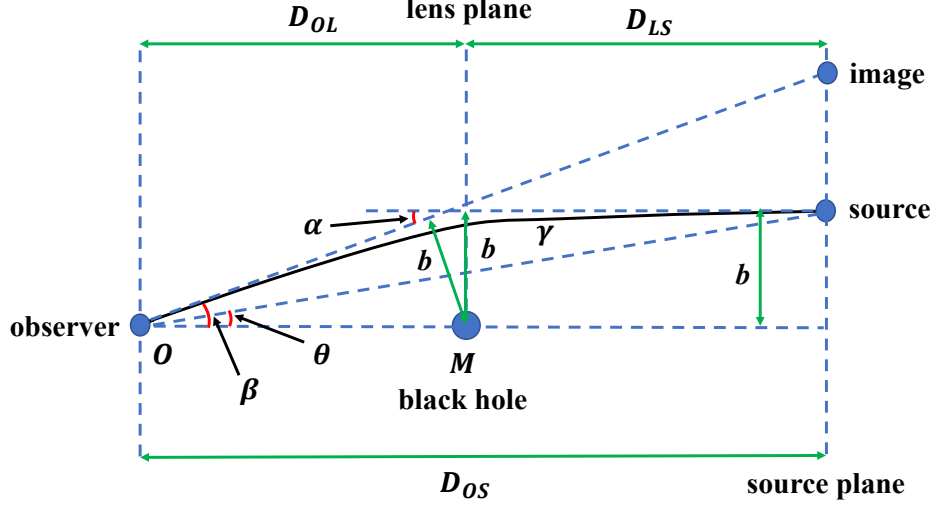


FIG. 3. Schematically plot of the weak gravitation lensing. The photon emitted by light source (luminous heavenly bodies) is lensed by central black hole. In this figure,  $D_{OS}$  is the distance between observer and source plane,  $D_{OL}$  is the distance between observer and lens plane,  $D_{LS}$  is the distance between lens plane and source plane. The central black hole is in the middle of lens plane. The angle  $\beta$  denotes the angular position of light source with respect to the optical axis  $OM$ , and  $\theta$  is the angular position of the lensed image seen by observer. The  $\alpha$  is the gravitational deflection angle of light, and  $b$  is the impact parameter.

### B. Weak Gravitational Lensing and Einstein Ring

As introduced in section I, acoustic black holes can be generated in many ways, not only from laboratory tabletop experiments in condensed matter systems, but also from mechanisms in high-energy physics and cosmology. If acoustic Schwarzschild black holes exist in our universe, they could be detected and observed from gravitational lensing observations.

In gravitational lensing observations, physical observables are mostly constrained by lens equation, which is given by [57–59]

$$D_{OS} \tan \beta = \frac{D_{OL} \sin \theta - D_{LS} \sin(\alpha - \theta)}{\cos(\alpha - \theta)} \quad (28)$$

Here,  $D_{OS}$  is the distance between observer and source plane,  $D_{OL}$  is the distance between observer and lens plane,  $D_{LS}$  is the distance between lens plane and source plane, the angles  $\beta$  and  $\theta$  are indicated in figure 3. It is worth noting that the angle  $\theta$  in lens equation is different from the angle  $\theta_i$  in Gauss-Bonnet theorem. In Gauss-Bonnet theorem,  $\theta_i$  is the exterior angle for each discontinuous point of boundary  $\partial D$ . However, the angle  $\theta$  in equation (28) is the angular position of the lensed image seen by observer. The images of the lensed objects (which are luminous heavenly bodies) can be achieved by solving lens equation (28). In the weak gravitational lensing, for distant source and observer, we have the approximations  $\tan \beta \approx \beta$ ,  $\sin \theta \approx \theta$ ,  $\sin(\alpha - \theta) \approx \alpha - \theta$  and

$\cos(\alpha - \theta) \approx 1$ . Then the lens equation (28) reduces to [60–62]

$$\beta = \theta - \frac{D_{LS}}{D_{OS}} \cdot \alpha \quad (29)$$

The relation  $D_{OS} = D_{OL} + D_{LS}$  has been used to derive this equation. The angular radius of Einstein ring is calculated by taking  $\beta = 0$ .

$$\begin{aligned} \theta_E &= \frac{D_{LS}}{D_{OS}} \cdot \alpha \\ &= \frac{D_{LS}}{D_{OS}} \cdot \left[ \frac{4M(1 + \xi)}{b} + \frac{3M^2(\xi^2 - 6\xi + 1)\pi}{4b^2} \right. \\ &\quad \left. + \frac{8M^3(\xi - 1)(\xi^2 - 4\xi - 1)}{3b^3} + o\left(\frac{M^4}{b^4}\right) \right] \end{aligned} \quad (30)$$

Further, in the weak gravitational lensing case, the impact parameter  $b$  satisfies

$$b \approx D_{OL} \sin \theta_E \approx D_{OL} \theta_E \quad (31)$$

Combining equation (30) and equation (31), the angular radius of Einstein ring  $\theta_E$  can be solved.

Although acoustic black holes could be generated by mechanisms in condensed matter physics, high-energy physics and cosmology. However, the realization of acoustic black holes only reported in condensed matter systems. There is no observational discoveries on astrophysical acoustic black holes so far. The experimental / observational constrains on its mass  $M$  and tuning parameter  $\chi$  are very weak. In this way, we can freely



TABLE I. Einstein ring of acoustic Schwarzschild black hole. The angular radii  $\theta_E$  of Einstein ring are presented for several tuning parameter  $\chi$ . In this table, the mass of acoustic Schwarzschild black hole is set as  $M = 4.3 \times 10^6 M_\odot$ , and the distances between observer, lens plane and source plane are chosen to be  $D_{LS} = D_{OS} = 8.3$  kpc<sup>a</sup>.

Tuning Parameter	Angular radius of Einstein ring
$\chi = 0$	$\theta_E = 1.45$ arcsec
$\chi = 0.2$	$\theta_E = 1.59$ arcsec
$\chi = 0.5$	$\theta_E = 1.78$ arcsec
$\chi = 1.0$	$\theta_E = 2.05$ arcsec
$\chi = 2.0$	$\theta_E = 2.51$ arcsec
$\chi = 5.0$	$\theta_E = 3.55$ arcsec

<sup>a</sup> We have excluded the unphysical solutions of Einstein ring  $\theta_E$  (namely when  $\theta_E$  gets complex values or negative values).

choose  $M = 4.3 \times 10^6 M_\odot$  and  $D_{LS} = D_{OL} = 8.3$  kpc, which are the mass and distance for Sgr A\*, as a representative example to show the Einstein ring of acoustic Schwarzschild black hole. To see the influence of tuning parameter on weak gravitational lensing, the angular radii of Einstein rings are calculated for several tuning parameters  $\xi$ , and the numerical results are presented in table I. From this table, it is notified that the Einstein ring of acoustic Schwarzschild black hole is larger than that of conventional Schwarzschild black hole. For larger tuning parameter  $\chi$ , the size of Einstein ring magnifies. Therefore, the acoustic black holes, with the presence of moving fluids and sound-waves, may be more easily detectable in weak gravitational lensing observations.

## V. SUMMARY

In this work, we study the gravitational bending effect of light in acoustic black hole. This category of black holes attracted broad research interests in recent years, for they open-up new directions for theoretical and experimental explorations of black holes. Some acoustic black holes could offer connections between dynamics of black holes and tabletop experiments in laboratories. The investigations on acoustic black holes may be beneficial for experimental explorations of black holes as well as theoretical analogue gravity models. To choose a simple and typical example, we consider the acoustic Schwarzschild black hole in this work. The acoustic Schwarzschild black hole could reflect some universal properties of more complex acoustic black holes, similar to the conventional Schwarzschild black hole. In this work, the gravitational deflection angle of light, weak gravitation lensing and Einstein ring of acoustic Schwarzschild black hole are discussed in details.

In the calculation of gravitational deflection angle, the Gauss-Bonnet theorem is applied in the optical manifold. In this approach, the gravitational bending effect is directly connected with the geometrical and topolog-

ical properties of curved spacetime (the geodesic curvature  $\kappa_g$ , Gauss curvature  $\mathcal{K}$ , and the Euler characteristic number  $\chi(D)$ ). In the calculations, the gravitational deflection angle  $\alpha$  is obtained from the integration of Gauss curvature in the equatorial plane of optical manifold. When the light source and observer are both located at infinite distance, the gravitational deflection angle for acoustic Schwarzschild black hole is expressed as

$$\alpha = \frac{4M(1+\xi)}{b} + \frac{3M^2(\xi^2 - 6\xi + 1)\pi}{4b^2} + \frac{8M^3(\xi - 1)(\xi^2 - 4\xi - 1)}{3b^3} + o\left(\frac{M^4}{b^4}\right) \quad (32)$$

When light source and observer are located at finite distance, the gravitational deflection angle is presented in the Appendix. The result for finite distance is consistent with the deflection angle in equation (32). Furthermore, when tuning parameter  $\xi = 0$ , equation (32) reduces to the gravitational deflection angle in conventional Schwarzschild black hole correctly ( $\alpha_{\text{Schwarzschild}} = 4M/b$ ). These observations could provide as confirmations for the validity of the approach used in the present work.

When tuning parameter  $\xi$  is nonzero, the gravitational bending in acoustic Schwarzschild black hole could be greatly different from conventional Schwarzschild black hole. Detailed calculations show that the gravitational deflection angle  $\alpha$  increases when tuning parameter  $\xi$  becomes larger. These results indicate that, compared with the conventional Schwarzschild black hole, the gravitational bending effect for acoustic Schwarzschild black hole is greatly enhanced.

From the weak gravitational lensing of acoustic Schwarzschild black hole, the angular radius of Einstein ring is solved through equation

$$\begin{aligned} \theta_E &= \frac{D_{LS}}{D_{OS}} \cdot \alpha \\ &= \frac{D_{LS}}{D_{OS}} \cdot \left[ \frac{4M(1+\xi)}{D_{OL}\theta_E} + \frac{3M^2(\xi^2 - 6\xi + 1)\pi}{4D_{OL}^2\theta_E^2} \right. \\ &\quad \left. + \frac{8M^3(\xi - 1)(\xi^2 - 4\xi - 1)}{3D_{OL}^3\theta_E^3} + o\left(\frac{M^4}{D_{OL}^4\theta_E^4}\right) \right] \quad (33) \end{aligned}$$

Numerical results indicate that the Einstein ring of acoustic Schwarzschild black hole is larger than that of conventional Schwarzschild black hole. And the size of Einstein ring magnifies for larger tuning parameter  $\chi$ . The acoustic black holes, with the presence of moving fluids and sound-waves, may be more easily detectable in gravitational bending and weak gravitational lensing observations.

The approach adopted in this work is general and model independent. It can be applied to arbitrary asymptotically flat acoustic black hole with spherical symmetry, such as the acoustic Reissner-Nordström black hole studied in [33]. We hope that the conclusions in this work could be useful for the theoretical and experimental investigations on acoustic black holes. We also hope

that this work could shed some light on the physics of black holes, as well as the analogue gravity models in high-energy physics and condensed matter physics.

### Appendix A: Gravitational Bending Effects for Acoustic Schwarzschild Black Hole — Light Source and Observer are Located at Finite Distance Region

In this appendix, we present results on gravitational bending of acoustic Schwarzschild black hole, with the finite distance effect taking into consideration. In this section, the locations of light source and observer are much different from the cases in section IV. Both light source and observer are not in the asymptotically flat region (infinite distance region). The distances between light source, observer and central massive object are finite.

To calculate the gravitational deflection angle of light for finite distance, we adopt the method developed by A. Ishihara *et al.* [36, 37]. This method is an extension of the Gibbons and Werner's work. In 2008, G. W. Gibbons and M. C. Werner first used Gauss-Bonnet theorem to calculate the gravitational deflection angle for the cases where light source and observer are located at infinity (the asymptotically flat region) [34]. In 2016-2017, A. Ishihara *et al.* extend this approach to the finite distance cases [36, 37]. In Ishihara's work, the gravitational deflection angle of light for finite distance is defined and calculated through

$$\alpha_{\text{finite distance}} = \Psi_{\text{source}} - \Psi_{\text{observer}} + \phi_{\text{OS}} \quad (\text{A1})$$

Here,  $\Phi_{\text{source}}$  and  $\Phi_{\text{observer}}$  are displayed in figure 4. The angle  $\phi_{\text{OS}}$  is the change of azimuthal angles

$$\phi_{\text{OS}} = \phi_{\text{observer}} - \phi_{\text{source}} \quad (\text{A2})$$

In the calculation of gravitational deflection angle for finite distance, the region  $D$  is chosen to be a simply connected region in the equatorial plane of optical manifold. The spacetime singularities are excluded from  $D$ , as illustrated in figure 4. For this region, the exterior angles for discontinuous points of boundary  $\partial D$  are:  $\theta_1 = \theta_2 = \pi/2$ ,  $\theta_{\text{observer}} = \Psi_{\text{observer}}$ ,  $\theta_{\text{source}} = \pi - \Psi_{\text{source}}$ . Therefore, the sum of exterior angles in Gauss-Bonnet theorem becomes

$$\begin{aligned} \sum_{i=1}^N \theta_i &= \theta_1 + \theta_2 + \theta_{\text{observer}} + \theta_{\text{source}} \\ &= 2\pi + \Psi_{\text{observer}} - \Psi_{\text{source}} \end{aligned} \quad (\text{A3})$$

The boundary  $\partial D$  in figure 4 consists of four parts: the photon orbit  $\gamma$ , the outer circular arc  $C_R$ , the lines  $L_1$  and  $L_2$ .  $L_1$  and  $L_2$  are lines for constant azimuthal angle  $\phi$ , and their geodesic curvature can be calculated through [55]

$$\kappa_g(L_1) = \kappa_g(L_2) = -\frac{1}{2\sqrt{\tilde{g}_{\phi\phi}^{\text{OP}}}} \frac{\partial \tilde{g}_{rr}^{\text{OP}}}{\partial \phi} = 0 \quad (\text{A4})$$

The photon orbit  $\gamma$  in gravitational field is a geodesic curve in optical geometry, so its geodesic curvature  $\kappa_g(\gamma)$  vanishes. Then the contour integral of geodesic curvature along boundary  $\partial D$  reduces to

$$\begin{aligned} \int_{\partial D} \kappa_g dl &= \int_{\gamma} \kappa_g(\gamma) dl + \lim_{R \rightarrow \infty} \int_{C_R} \kappa_g(C_R) dl \\ &\quad + \int_{L_1} \kappa_g(L_1) dl + \int_{L_2} \kappa_g(L_2) dl \\ &= \lim_{R \rightarrow \infty} \int_{C_R} \kappa_g(C_R) dl \end{aligned} \quad (\text{A5})$$

For the circular arc curve  $C_R$ , the geodesic curvature has been given in equation (20). Therefore, the integration of geodesic curvature  $\kappa_g$  along the boundary  $\partial D$  becomes

$$\begin{aligned} \int_{\partial D} \kappa_g dl &= \lim_{R \rightarrow \infty} \int_{C_R} \kappa_g(C_R) dl \\ &= \lim_{R \rightarrow \infty} \int_{\phi_{\text{source}}}^{\phi_{\text{observer}}} \kappa_g(C_R) R d\phi \\ &= \lim_{R \rightarrow \infty} \int_{\phi_{\text{source}}}^{\phi_{\text{observer}}} \left[ \frac{1}{R} - \frac{3M(1+\xi)}{R^2} \right. \\ &\quad \left. + \frac{16M^2\xi}{R^3} - \frac{20M^3\xi}{R^4} \right] R d\phi \\ &= \phi_{\text{observer}} - \phi_{\text{source}} \\ &= \phi_{\text{OS}} \end{aligned} \quad (\text{A6})$$

Combining the exterior angles in equation (A3), contour integral of geodesic curvature in equation (A6) and Euler characteristic number  $\chi(D) = 1$ , the Gauss-Bonnet theorem in equation (1) leads to

$$\begin{aligned} \int_D \mathcal{K} dS + \int_{\partial D} \kappa_g dl + \sum_{i=1}^N \theta_i \\ = \int_D \mathcal{K} dS + \phi_{\text{OS}} + (2\pi + \Psi_{\text{observer}} - \Psi_{\text{source}}) \\ = 2\pi\chi(D) = 2\pi \end{aligned} \quad (\text{A7})$$

Therefore, in the asymptotically flat spacetime, the gravitational deflection angle of light for finite distance can be calculated through

$$\begin{aligned} \alpha_{\text{finite distance}} &= \Psi_{\text{source}} - \Psi_{\text{observer}} + \phi_{\text{OS}} \\ &= - \int_D \mathcal{K} dS \\ &= - \int_{\phi_{\text{source}}}^{\phi_{\text{observer}}} d\phi \int_{r(\gamma)}^{\infty} \mathcal{K} \frac{r}{[f(r)]^{3/2}} dr \end{aligned} \quad (\text{A8})$$

This is the gravitational deflection angle of light in cases where observer and light source are both from finite distance region.

The same as in subsection IV A, the radius of photon orbit  $r(\gamma) = r(\phi)$  must be determined to evaluate the integration of Gauss curvature. To avoid solving complicated differential equations for null geodesic, we can use

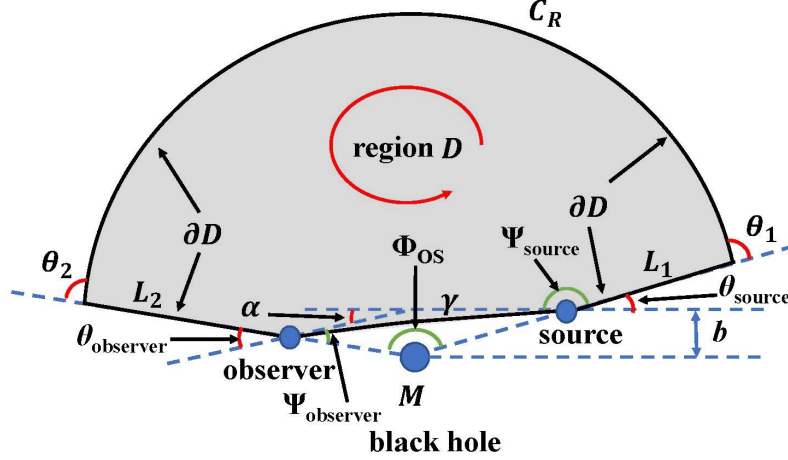


FIG. 4. Calculating the gravitational deflection angle of light for finite distance using Gauss-Bonnet theorem. This figure shows the choice of region  $D$  in the equatorial plane of optical manifold in cases where light source and observer are both from finite distance region. This region  $D$  would make the application of Gauss-Bonnet theorem in equation (1) available in the calculation of gravitational deflection angle. The direction of boundary  $\partial D$  in contour integral  $\int_{\partial D} \kappa_g dl$  is chosen to be counterclockwise. Note that for photon orbit  $\gamma$ , this choice of direction (which is from observer to light source) is opposite to the light propagation. In this figure,  $\Psi_{\text{source}}$  and  $\Psi_{\text{observer}}$  are the angles between photon orbit  $\gamma$  and radial direction, which are exactly the definitions in Ishihara's work [36]. The angle  $\phi_{\text{OS}} = \phi_{\text{observer}} - \phi_{\text{source}}$  is the change of azimuthal angles. After these definitions, the gravitational deflection angle of light for finite distance can be expressed as  $\alpha_{\text{finite distance}} = \Psi_{\text{source}} - \Psi_{\text{observer}} + \phi_{\text{OS}}$ .

the leading order perturbation for photon orbit, which is the photon orbit in Newtonian gravity. Namely,

$$r(\gamma) = r(\phi) \approx \frac{b}{\sin \phi} \quad (\text{A9})$$

Plug the Gauss curvature in equation (18), surface area in equation (19) and the photon orbit in equation (A9) into the integration (A8), finally we can obtain

$$\begin{aligned}
 \alpha_{\text{finite distance}} &= - \int_D \mathcal{K} dS = - \int_{\phi_{\text{source}}}^{\phi_{\text{observer}}} d\phi \int_{r(\gamma)}^{\infty} \mathcal{K} \frac{r}{[f(r)]^{3/2}} dr \\
 &\approx - \int_{\phi_{\text{source}}}^{\phi_{\text{observer}}} d\phi \int_{\frac{b}{\sin \phi}}^{\infty} \mathcal{K} \frac{r}{[f(r)]^{3/2}} dr \\
 &= - \int_{\phi_{\text{source}}}^{\phi_{\text{observer}}} d\phi \int_{\frac{b}{\sin \phi}}^{\infty} \left[ -\frac{2M(1+\xi)}{r^2} - \frac{3M^2(\xi^2 - 6\xi + 1)}{r^3} - \frac{6M^3(\xi - 1)(\xi^2 - 4\xi - 1)}{r^4} + o\left(\frac{M^4}{r^5}\right) \right] dr \\
 &= \int_{\phi_{\text{source}}}^{\phi_{\text{observer}}} \left[ \frac{2M(1+\xi) \sin \phi}{b} + \frac{3M^2(\xi^2 - 6\xi + 1) \sin^2 \phi}{2b^2} + \frac{2M^3(\xi - 1)(\xi^2 - 4\xi - 1) \sin^3 \phi}{b^3} + o\left(\frac{M^4}{b^4}\right) \right] d\phi \\
 &= \frac{2M(1+\xi)}{b} \left[ \cos(\phi_{\text{source}}) - \cos(\phi_{\text{observer}}) \right] \\
 &\quad + \frac{3M^2(\xi^2 - 6\xi + 1)}{4b^2} \left[ \cos(\phi_{\text{source}}) \sin(\phi_{\text{source}}) - \cos(\phi_{\text{observer}}) \sin(\phi_{\text{observer}}) + \phi_{\text{OS}} \right] \\
 &\quad + \frac{2M^3(\xi - 1)(\xi^2 - 4\xi - 1)}{3b^3} \left\{ [2 + \sin^2(\phi_{\text{source}})] \cdot \cos(\phi_{\text{source}}) - [2 + \sin^2(\phi_{\text{observer}})] \cdot \cos(\phi_{\text{observer}}) \right\} \\
 &\quad + o\left(\frac{M^4}{b^4}\right) \quad (\text{A10})
 \end{aligned}$$

To solve the azimuthal angles  $\phi_{\text{source}}$  and  $\phi_{\text{observer}}$  approximately in a simpler way, we also employ the leading order

solution for photon orbit

$$r(\gamma) \approx \frac{b}{\sin \phi} \Rightarrow \sin \phi \approx \frac{b}{r} = bu \quad (\text{A11})$$

Recall that the azimuthal angle in figure 4 satisfies  $\phi_{\text{source}} < \pi/2$  and  $\phi_{\text{observer}} > \pi/2$ . The trigonometric functions become

$$\cos(\phi_{\text{source}}) = \sqrt{1 - b^2 u_{\text{source}}^2} \quad (\text{A12a})$$

$$\cos(\phi_{\text{observer}}) = -\sqrt{1 - b^2 u_{\text{observer}}^2} \quad (\text{A12b})$$

Finally, the gravitational deflection angle of light can be expressed as

$$\begin{aligned} \alpha_{\text{finite distance}} = & \frac{2M(1+\xi)}{b} [\sqrt{1 - b^2 u_{\text{source}}^2} + \sqrt{1 - b^2 u_{\text{observer}}^2}] + \frac{3M^2(\xi^2 - 6\xi + 1)}{4b^2} \\ & \cdot \left[ bu_{\text{source}} \sqrt{1 - b^2 u_{\text{source}}^2} + bu_{\text{observer}} \sqrt{1 - b^2 u_{\text{observer}}^2} + \pi - \arcsin(bu_{\text{observer}}) - \arcsin(bu_{\text{source}}) \right] \\ & + \frac{2M^3(\xi - 1)(\xi^2 - 4\xi - 1)}{3b^3} \cdot \left[ (2 + b^2 u_{\text{source}}^2) \sqrt{1 - b^2 u_{\text{source}}^2} + (2 + b^2 u_{\text{observer}}^2) \sqrt{1 - b^2 u_{\text{observer}}^2} \right] \\ & + o\left(\frac{M^3}{b^3}\right) \end{aligned} \quad (\text{A13})$$

This is the gravitational deflection angle in acoustic Schwarzschild black hole where light source and observer are both from finite distance region.

The gravitational deflection angle in acoustic Schwarzschild black hole for finite distance in equation (A13) is consistent with the results presented in subsection IV A. When observer and light source are both located at infinite distance, which correspond to the case in subsection IV A, we have

$$r_{\text{source}} \rightarrow \infty \Rightarrow u_{\text{source}} = 1/r_{\text{source}} \rightarrow 0 \quad (\text{A14a})$$

$$r_{\text{observer}} \rightarrow \infty \Rightarrow u_{\text{observer}} = 1/r_{\text{observer}} \rightarrow 0 \quad (\text{A14b})$$

Plugging these relations into equation (A13), the gravitational deflection angle becomes

$$\begin{aligned} \alpha \rightarrow & \frac{4M(1+\xi)}{b} + \frac{3M^2(\xi^2 - 6\xi + 1)\pi}{4b^2} \\ & + \frac{8M^3(\xi - 1)(\xi^2 - 4\xi - 1)}{3b^3} + o\left(\frac{M^4}{b^4}\right) \end{aligned} \quad (\text{A15})$$

In this case, the above results reduces to the gravitational deflection angle of light calculated in equation (26).

## ACKNOWLEDGMENTS

We acknowledge helpful discussions with Peng Wang, Xing-Da Liu and Ming Li. Chen-Kai Qiao thanks Lin Wang for kindly support and encouragement. The authors should thank to the great efforts from all around the world during the pandemic period of COVID-19. This work was supported by the the Scientific Research Foundation of Chongqing University of Technology (Grants No. 2020ZDZ027), and the Natural Science Foundation of Chongqing (Grant No. cstc2020jcyj-msxmX0879).

- [1] F. W. Dyson, A. S. Eddington and C. Davidson, *A Determination of the Deflection of Light by the Sun's Gravitational Field, from Observations Made at the Total Eclipse of May 29, 1919*. *Phil. Trans. R. Soc. Lond. A* **220**, 291-333 (1920).
- [2] J. Wambsganss, *Gravitational Lensing in Astronomy*, *Living Rev. Relativ.* **1**, 12 (1998).
- [3] M. Bartelmann and P. Schneider, *Weak gravitational lensing*, *Phys. Rept.* **340**, 291-472 (2001).
- [4] E. van Uitert, H. Hoekstra, T. Schrabback, D. G.

- Gilbank, M. D. Gladders and H. K. C. Yee, *Constraints on the shapes of galaxy dark matter haloes from weak gravitational lensing*, *Astron. Astrophys.* **545**, A71 (2012). [arXiv:1206.4304\[astro-ph.CO\]](#)
- [5] K. S. Virbhadra and George F. R. Ellis, *Schwarzschild black hole lensing*, *Phys. Rev. D* **62**, 084003 (2000). [arXiv:9904193\[astro-ph\]](#)
- [6] *Black Hole Physics*, edited by V. de Sabbata and Z.-J. Zhang (Springer, Netherlands, 1992). [doi:10.1007/978-94-011-2420-1](#)

- [7] B Abbott, R Abbott, T D Abbott, *et al.* (LIGO Scientific Collaboration and Virgo Collaboration) *Observation of Gravitational Waves from a Binary Black Hole Merger*, *Phys. Rev. Lett.* **116**, 061102 (2016).
- [8] K. Akiyama *et al.* (Event Horizon Telescope Collaboration), *First M87 Event Horizon Telescope Results. I. The Shadow of the Supermassive Black Hole*, *Astrophys. J.* **875**, L1 (2019). [arXiv:1906.11238 \[astro-ph.GA\]](#)
- [9] W. G. Unruh, *Experimental Black-Hole Evaporation*, *Phys. Rev. Lett.* **46**, 1351-1353 (1981).
- [10] C. Barcelo, S. Liberati and M. Visser, *Analogue Gravity*, <https://doi.org/10.12942/lrr-2005-12> *Living Rev. Rel.* **8**, 12 (2005). [arXiv:0505065\[gr-qc\]](#)
- [11] M. Visser, *Acoustic black holes: Horizons, Ergospheres, and Hawking radiation*, *Class. Quantum Grav.* **15**, 1767-1791 (1998). [arXiv:9712010\[gr-qc\]](#)
- [12] M. Visser, *Acoustic black holes*, 1999. [arXiv:9901047\[gr-qc\]](#)
- [13] C. Barceló, *Analogue black-hole horizons*, *Nature Phys.* **15**, 210-213 (2019).
- [14] O. Lahav, A. Itah, A. Blumkin, C. Gordon, and J. Steinhauer, *Realization of a Sonic Black Hole Analogue in a Bose-Einstein Condensate*, *Phys. Rev. Lett.* **105**, 240401 (2010). [arXiv:0906.1337\[cond-mat.quant-gas\]](#)
- [15] J. Steinhauer, *Observation of self-amplifying Hawking radiation in an analog black hole laser*, *Nature Phys.* **10**, 864-869 (2014). [arXiv:1409.6550\[cond-mat.quant-gas\]](#)
- [16] J. Drori, Y. Rosenberg, D. Bermudez, Y. Silberberg and U. Leonhardt, *Observation of Stimulated Hawking Radiation in an Optical Analogue*, *Phys. Rev. Lett.* **122**, 010404 (2019). [arXiv:1808.09244\[gr-qc\]](#)
- [17] M. P. Blencowe and H. Wang, *Analogue Gravity on a Superconducting Chip*, *Phil. Trans. Roy. Soc. Lond. A* **378**, 20190224 (2020). [arXiv:2003.00382\[quant-ph\]](#)
- [18] B. W. Drinkwater, *An acoustic black hole*, *Nat. Phys.* **16**, 1010-1011 (2020).
- [19] J. R. M. de Nova, K. Golubkov, V. I. Kolobov, and J. Steinhauer, *Observation of thermal Hawking radiation and its temperature in an analogue black hole*, *Nature* **569**, 688-691 (2019).
- [20] M. Isoard and N. Pavloff, *Departing from Thermal-ity of Analogue Hawking Radiation in a Bose-Einstein Condensate*, *Phys. Rev. Lett.* **124**, 060401 (2020). [arXiv:1909.02509\[cond-mat.quant-gas\]](#)
- [21] X.-H. Ge and S.-J. Sin, *Acoustic black holes for relativistic fluids*, *JHEP* **2010(06)**, 087 (2010). [arXiv:1001.0371\[hep-th\]](#)
- [22] M. Anacleto, F. Brito, and E. Passos, *Acoustic black holes from Abelian Higgs model with Lorentz symmetry breaking*, *Phys. Lett. B* **694**, 149-157 (2010). [arXiv:1004.5360\[hep-th\]](#)
- [23] C. Yu and J.-R. Sun, *Note on acoustic black holes from black D3-brane*, *Int. J. Mod. Phys. D* **28**, 1950095 (2019). [arXiv:1712.04137 \[hep-th\]](#)
- [24] X.-H. Ge, M. Nakahara, S.-J. Sin, Y. Tian, and S.-F. Wu, *Acoustic black holes in curved spacetime and the emergence of analogue Minkowski spacetime*, *Phys. Rev. D* **99**, 104047 (2019). [arXiv:1902.11126\[hep-th\]](#)
- [25] U. R. Fischer and M. Visser, *Riemannian Geometry of Irrotational Vortex Acoustics*, *Phys. Rev. Lett.* **88**, 110201 (2002). [arXiv:0110211\[cond-mat\]](#)
- [26] U. R. Fischer and M. Visser, *On the space-time curvature experienced by quasiparticle excitations in the Painlevé-Gullstrand effective geometry*, *Annals Phys.* **304**, 22-39 (2003). [arXiv:0205139\[cond-mat\]](#)
- [27] V. Cardoso, J. P. S. Lemos and S. Yoshida, *Quasinormal modes and stability of the rotating acoustic black hole: Numerical analysis*, *Phys. Rev. D* **70**, 124032 (2004). [arXiv:0410107\[gr-qc\]](#)
- [28] C. L. Benone, L. C. B. Crispino, C. Herdeiro and E. Radu, *Acoustic clouds: standing sound waves around a black hole analogue*, *Phys. Rev. D* **91**, 104038 (2015). [arXiv:1412.7278\[gr-qc\]](#)
- [29] C. A. U. Lima, F. Brito, J. A. Hoyos and D. A. T. Vanzella, *Probing the Unruh effect with an accelerated extended system*, *Nature Communications* **10**, 3030 (2019). [arXiv:1805.00168\[gr-qc\]](#)
- [30] G. Eskin, *New examples of Hawking radiation from acoustic black holes*, 2019. [arXiv:1906.06038\[math-ph\]](#)
- [31] H. Guo, H. Liu, X. -M. Kuang, and B. Wang, *Acoustic black hole in Schwarzschild spacetime: Quasinormal modes, analogous Hawking radiation, and shadows*, *Phys. Rev. D* **102**, 124019 (2020). [arXiv:2007.04197\[gr-qc\]](#)
- [32] H. S. Vieira, Kostas D. Kokkotas, *Quasibound states of Schwarzschild acoustic black holes*, *Phys. Rev. D* **104**, 024035 (2021). [arXiv:2104.03938\[gr-qc\]](#)
- [33] R. Ling, H. Guo, H. Liu, X. -M. Kuang and B. Wang, *Shadow and near-horizon characteristics of the acoustic charged black hole in curved spacetime*, 2021. [arXiv:2107.05171\[gr-qc\]](#)
- [34] G. W. Gibbons and M. C. Werner, *Applications of the Gauss-Bonnet theorem to gravitational lensing*, *Class. Quantum Grav.* **25**, 235009 (2008). [arXiv:0807.0854\[gr-qc\]](#)
- [35] M. C. Werner, *Gravitational lensing in the Kerr-Randers optical geometry*, *Gen. Relativ. Gravit.* **44**, 3047-3057 (2012). [arXiv:1205.3876\[gr-qc\]](#)
- [36] A. Ishihara, Y. Suzuki, T. Ono, T. Kitamura, and H. Asada, *Gravitational bending angle of light for finite distance and the Gauss-Bonnet theorem*, *Phys. Rev. D* **94**, 084015 (2016). [arXiv:1604.08308\[gr-qc\]](#)
- [37] A. Ishihara, Y. Suzuki, T. Ono and H. Asada, *Finite-distance corrections to the gravitational bending angle of light in the strong deflection limit*, *Phys. Rev. D* **95**, 044017 (2017). [arXiv:1612.04044\[gr-qc\]](#)
- [38] A. Övgün, I. Sakalli and J. Saavedra, *Shadow cast and deflection angle of Kerr-Newman-Kasuya spacetime*, *JCAP* **2018(10)**, 041 (2018). [arXiv:1807.00388\[gr-qc\]](#)
- [39] K. Jusufi, A. Övgün, J. Saavedra, Y. Vásquez and P. A. González, *Deflection of light by rotating regular black holes using the Gauss-Bonnet theorem*, *Phys. Rev. D* **97**, 124024 (2018). [arXiv:1804.00643\[gr-qc\]](#)
- [40] G. Crisnejo, E. Gallo and A. Rogers, *Finite distance corrections to the light deflection in a gravitational field with a plasma medium*, *Phys. Rev. D* **99**, 124001 (2019). [arXiv:1807.00724\[gr-qc\]](#)
- [41] K. Takizawa, T. Ono, and H. Asada, *Gravitational deflection angle of light: Definition by an observer and its application to an asymptotically nonflat spacetime*, *Phys. Rev. D* **101**, 104032 (2020). [arXiv:2001.03290\[gr-qc\]](#)
- [42] R. C. Pantig and E. T. Rodulfo, *Weak deflection angle of a dirty black hole*, *Chinese J. Phys.* **66**, 691-702 (2020). [arXiv:2003.00764\[gr-qc\]](#)
- [43] Qi-Ming Fu, Li Zhao and Yu-Xiao Liu, *Weak deflection angle by electrically and magnetically charged black holes from nonlinear electrodynamics*, *Phys. Rev. D* **104**, 024033 (2021). [arXiv:2101.08409\[gr-qc\]](#)



- [44] W. Javed, M. B. Khadim and A. Övgün, *Weak gravitational lensing by Bocharova-Bronnikov-Melnikov-Bekenstein black holes using Gauss-Bonnet theorem*, *Eur. Phys. J. Plus* **135**, 595 (2020). [arXiv:2007.14844\[gr-qc\]](#)
- [45] G. Crisnejo and E. Gallo, *Weak lensing in a plasma medium and gravitational deflection of massive particles using the Gauss-Bonnet theorem. A unified treatment*, *Phys. Rev. D* **97**, 124016 (2018). [arXiv:1804.05473\[gr-qc\]](#)
- [46] G. Crisnejo, E. Gallo and K. Jusufi, *Higher order corrections to deflection angle of massive particles and light rays in plasma media for stationary spacetimes using the Gauss-Bonnet theorem*, *Phys. Rev. D* **100**, 104045 (2019). [arXiv:1910.02030\[gr-qc\]](#)
- [47] Z. -H. Li, G. -S. He and T. Zhou, *Gravitational deflection of relativistic massive particles by wormholes*, *Phys. Rev. D* **101**, 044001 (2020). [arXiv:1908.01647\[gr-qc\]](#)
- [48] Z. -H. Li, J. -J. Jia, *The finite-distance gravitational deflection of massive particles in stationary spacetime: a Jacobi metric approach*, *Eur. Phys. J. C* **80**, 157 (2020). [arXiv:1912.05194\[gr-qc\]](#)
- [49] S. -S. Chern, W. -H. Chern and K. S. Lam, *Lectures on Differential Geometry* (World Scientific Publishing, Singapore, 1999).
- [50] M. A. Abramowicz, B. Carter and J. P. Lasota, *Optical reference geometry for stationary and static dynamics*, *Gen. Relat. Gravit.* **20**, 1173–1183 (1988).
- [51] G.W. Gibbons and C. M. Warnick, *Universal properties of the near-horizon optical geometry*, *Phys. Rev. D* **79**, 064031 (2009). [arXiv:0809.1571\[gr-qc\]](#)
- [52] W. Javed, J. Abbas and A. Övgün, *Deflection angle of photon from magnetized black hole and effects of non-linear electrodynamics*, *Eur. Phys. J. C* (2019) **79**, 694 (2019). [arXiv:1908.09632\[physics.gen-ph\]](#)
- [53] K. Jusufi, *Determining the Topology and Deflection Angle of Ringholes via Gauss-Bonnet Theorem*, *Universe* **7**, 44 (2021). [arXiv:1807.09748\[gr-qc\]](#)
- [54] E. P. Gross, *Structure of a quantized vortex in boson systems*, *Nuovo Cim* **20**, 454-477 (1961).
- [55] W. -H. Chern, *Differential Geometry* (Peking University Press, Beijing, 2006).
- [56] There is a point worth noting. For higher order series of  $M/b$ , the gravitational deflection angle for conventional Schwarzschild spacetime obtained in our work (correspond to  $\xi = 0$  in equation (26)) is not consistent with the result in reference [58]. This is due to the approximations of photon orbit  $r(\gamma) = r(\phi)$  used in the integration of Gauss curvature. In this work, we adopt the leading order approximation for photon orbit.
- $$r(\gamma) = r(\phi) \approx \frac{b}{\sin \phi} \Rightarrow b \approx \frac{\sin \phi}{u}$$
- However, in reference [58], a higher order approximation for photon orbit was used in the integration.
- $$b \approx \frac{\sin \phi}{u} + \frac{M(1 - \cos \phi)^2}{u^2} - \frac{M^2(60\phi \cos \phi + 3 \sin 3\phi - 5 \sin \phi)}{16u^3}$$
- Here,  $u = 1/r(\gamma)$ .
- [57] V. Bozza, *Comparison of approximate gravitational lens equations and a proposal for an improved new one*, *Phys. Rev. D* **78**, 103005 (2008). [arXiv:0807.3872\[gr-qc\]](#)
- [58] S. U. Islam, R. Kumar and S. G. Ghosh, *Gravitational lensing by black holes in the 4D Einstein-Gauss-Bonnet gravity*, *JCAP* **2020(09)**, 030 (2020). [arXiv:2004.01038\[gr-qc\]](#)
- [59] F. Atamurotov, U. Papnoi and K. Jusufi, *Shadow and deflection angle of charged rotating black hole surrounded by perfect fluid dark matter*, 2021. [arXiv:2104.14898\[gr-qc\]](#)
- [60] V. Bozza, S. Capozziello, G. Iovane and G. Scarpetta, *Strong field limit of black hole gravitational lensing*, *Gen. Rel. Grav.* **33**, 1535-1548 (2001). [arXiv:0102068\[gr-qc\]](#)
- [61] A. O. Petters, H. Levine, and J. Wambsganss, *Singularity Theory and Gravitational Lensing* (Birkhäuser, Boston, 2001). [doi:10.1007/978-1-4612-0145-8](#)
- [62] S. Mollerach and E. Roulet, *Gravitational Lensing and Microlensing* (World Scientific, Singapore, 2002).